Prediction of membrane fouling rate by neural network modeling

Tae-Mun Hwang[a,b]*, Yongjun Choi[c], Sook-Hyun Nam[a], Sangho Lee[a], Hyunje Oh[a,b],
Kyounghak Hyun[b], Youn-Kyoo Choung[b]

[a]*Korea Institute of Construction Technology, 2311 Daehwa-Dong, Ilsan-gu, Kyonggi-do, Korea*
[b]*Department of Civil and Environmental Engineering, Yonsei University, Sinchondong 134, Sudaemungu, Seoul 120-749, Korea*
Tel. +82 (31) 910-0741; Fax +82 (31) 910-0291; email: taemun@kict.re.kr
[c]*University of Science & Technology, 113 Gwahangno, Uuseong-Gu, Daejeon 305-333, Korea*

ABSTRACT

Cross-flow microfiltration is an efficient and energy-saving method for separating fine particles from liquids in many chemical, environmental, biochemical and materials processes. Although this filtration mode has many advantages, the flux decline at a constant pressure, or similarly, the transmembrane pressure increase at constant flux due to membrane fouling is a severe barrier to its further development and wide application. The objective of this research was to identify the seasonal characteristics of the raw water collected from the Han River, and to develop a model that can predict and/or monitor the fouling rate. An MLP (multi-layer perceptron) employing the sigmoid transfer function and the back propagation algorithm for training was constructed with the STATISTICA. The ANN input parameters were carefully selected to include the physically meaningful and easy-to-measure membrane operations. The results of the experiment indicated that the seasonal variations in the raw water quality parameters significantly affected the membrane fouling rate. The comparison of the ANN model calculations with the experiment results revealed that the ANN model is a useful tool for predicting the membrane fouling characteristics.

Keywords: Artificial neural network; Microfiltration; Fouling rate; Cake filtration

1. Introduction

Microfiltration is a particularly efficient technique for separating particles ranging from 0.1 µm up to a few microns in size from a liquid medium [1]. It can be conducted using two distinct modes of operation, referred to as dead-end microfiltration and cross-flow microfiltration. In the dead-end configuration, the feed suspension flows perpendicular to the membrane surface, whereas in cross-flow systems, the suspension flow is tangential to the membrane [2]. Cross-flow microfiltration is an efficient and antifouling method for separating fine particles from liquids in many chemical, environmental, biochemical and materials processes. Although this filtration mode has many advantages, the flux decline at a constant pressure, or similarly, the transmembrane pressure increase at constant flux due to membrane fouling is a severe barrier to its further development and wide application [3]. Membrane fouling is responsible for the non-steady state of the membrane process as it causes permeate flux decline with the passage of time. For this reason, the steady-state flux decline models are not capable of accurately describing membrane performance in the membrane process. It is thus necessary to use the non-steady-state model for this purpose. Recently, several studies have been conducted

---

* Corresponding author.

to predict membrane performance using artificial neural networks (ANNs) [4,5]. The artificial neural network is an effective predictive method for modeling the behavior of nonlinear dynamic systems.

The objectives of this research were to identify the seasonal characteristics of the raw water collected from the Han River and to develop a model that can predict and/or monitor the fouling rate for better fouling control and for the reduction of membrane fouling under constant flux using the artificial neural network.

2. Theory

2.1. Membrane fouling rate

Microfiltration membranes are designed to remove particulates from water via a sieving mechanism. Therefore, particle fouling, the deposition of colloids and suspended solids on membranes remains a common phenomenon in MF systems. It is thus necessary to develop the fouling rate to predict and/or monitor membrane fouling for better fouling control.

During filtration, when the particles are larger than the pores, they are removed on the surface as a cake. During unstirred filtration at a constant pressure under conditions of perfect retention, the following expression can be derived, relating the cumulative filtrate volume V to the filtration time t [6].

$$\frac{t}{V} = \frac{\mu R_m}{A\Delta P} + \frac{\mu\alpha C_0 V}{2A^2\Delta P} \tag{1}$$

where A is the membrane surface area, μ the absolute viscosity, ΔP the transmembrane pressure, C_o the feed water particle concentration, and α the specific cake resistance on a mass basis. $\alpha C_0/10^{12}$ was used in this study as a membrane fouling rate. The fouling rate can also be determined in constant-flux filtration. The resistance-in-

series model was applied under constant flux. Only a broad outline of the model is given in Table 1 since the details were provided separately [7].

The fouling rate can be determined from the slope of the linear region in a plot of ΔP vs. time, which corresponds to cake filtration or the manipulation of Eq. (5).

2.2. Artificial neural networks (ANN)

An artificial neural network is a nonlinear statistical data modeling tool inspired by the way biological nervous systems, such as the brain, process information. It consists of an interconnected group of artificial neurons and processes information using a connectionist approach to computation. In most cases, an ANN is an adaptive system that changes its structure based on the external or internal information that flows through the network during the learning phase. It can be used to model the complex relationships between the inputs and the outputs, or to find patterns in data. An artificial neural network consists of a collection of processing elements that are highly interconnected and that transform a set of inputs into a set of desired outputs. The result of the transformation is determined by the characteristics of the elements and the weights associated with the interconnections among them. By modifying the connections between the nodes, the network is able to adapt to the desired outputs [8,9].

An ANN model for predicting the membrane fouling rate and permeability using a multilayer perceptron network (MLP) with a back propagation (BP) training algorithm was used in this study. MLP is useful in research due to its ability to solve problems stochastically, which often allows one to obtain approximate solutions for extremely complex problems like fitness approximation. A multilayer feed forward neural-network architecture is shown in Fig. 1. A multilayer perceptron is a feedforward artificial neural network model that maps sets of input

Table 1
Summary of the model equations for the fouling rate in constant flux

Meaning	Model equation	
Flux through a resistance-in-series approach	$J = \dfrac{\Delta P}{\mu(R_m + R_c)}$	(2)
Cake resistance	$R_c = \dfrac{V}{A}\alpha C_0$	(3)
Substitution of Eq. (3) into Eq. (2)	$J = \dfrac{\Delta P}{\mu\left(R_m + \dfrac{V}{A}\alpha C_0\right)}$	(4)
Rewriting V/A as Jt and rearranging it gives the following equation	$\Delta P = J\mu R_m + J^2\mu It$	(5)
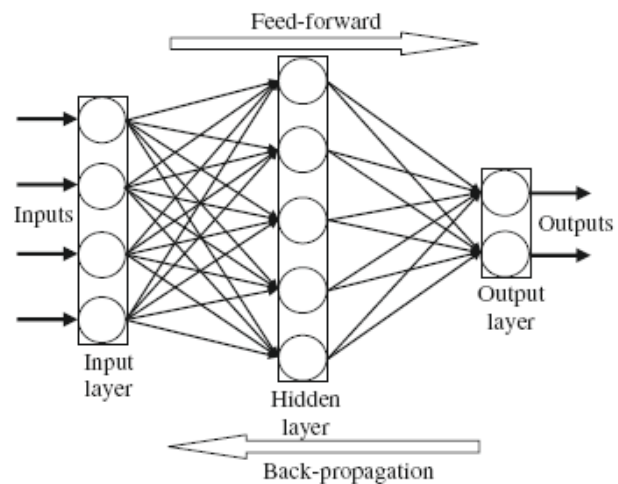
Fig. 1. Schematic diagram of a multilayer feed forward neural network.

data onto a set of appropriate outputs. It is a modification of the standard linear perceptron in that it uses three or more layers of neurons (nodes) with nonlinear activation functions.

3. Materials and methods

3.1. Pilot scale membrane system

Fig. 2 illustrates the schematic diagram of a pilot plant (500 m³/d) for this study. The pilot-scale pressurized membrane filtration system was composed of a rapid mixing/coagulation/sedimentation process and filtration using PVDF membranes (H2L, Korea). Raw water collected from the Han River was used in this study as feed water after coagulation and sedimentation pretreatment using polyaluminum chloride (17%).

The specifications of the membrane are summarized in Table 2. The operation conditions are as follows: 40-min filtration, 30-s backwash with permeate and 1-min backwash with pressurized air. The system was automatically operated, and the data were collected using a computer.

3.2. ANN model establishment

Two ANN models were developed in this study to predict the fouling rate and permeability. An MLP employing the sigmoid transfer function and the back propagation algorithm for training was constructed with STATISTICA. The ANN input parameters were carefully

selected to include the physically meaningful and easy-to-measure membrane operations. The ANN model used input parameters for the operation conditions (coagulant dosage, operating time) and water quality (raw water turbidity, raw water pH, total algae number of the raw water). A total of 6,400 data samples were divided into 5,120 training samples and 1,280 test samples. The neural-network predictions were quantitatively evaluated using the root mean squared error (RMSE) and absolute fraction of variance (R^2).

$$\text{RMSE} = \sqrt{\frac{\sum_N (t_i - O_i)^2}{N}} \tag{6}$$

$$R^2 = \left(\frac{(n\sum t_i O_i - \sum t_i \sum O_i)^2}{(n\sum t_i^2 - (n\sum t_i)^2(n\sum O_i^2 - (n\sum O_i)^2)} \right) \tag{7}$$

where t is the predicted value, O the observed value, i is the sample number and n the pattern.

4. Results and discussion

4.1. Raw water quality

Fig. 3 shows the variation in the quality of the raw water that was used for membrane filtration. The turbidity, total algae number, and TOC in the raw water significantly changed with time. The TOC was high in winter (from January to February), and the algae number was high in spring (from March to May). In summer (from June to August), the raw water turbidity remained high due to frequent rains.

The characteristics of raw water quality are summarized in Table 3. The turbidity, total organic carbon, algae number, and temperature of the feed water were 2.02–150.00 NTU, 1.43–6.94 mg/L, 306–27,080 cell/mL, and 1.16–25.89°C, respectively. The seasonal difference in the raw water quality suggests that the filtration characteristics may be quite different.

4.2. Fouling rate

The fouling rate was calculated based on the 40-min filtration cycle, using the inclination of the straight line within the filtration time and the transmembrane pressure graph. The fouling rate was determined from the

Table 2
Specifications of the hollow fiber membrane

Item	Content
Membrane material	PVDF
Module type	Hollow fiber
Pore size, μm	0.1
Operation mode	Pressurized type
Filtration mode	Constant flow rate
Surface area, m²	50
Interval of physical cleaning, min	40
Filtration method	Cross-flow
Flow type	Outside-in

Raw water   Coagulation/Sedimentation   MF   GAC
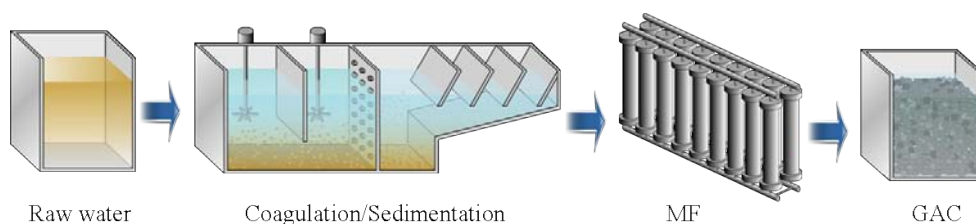
Fig. 2. Schematic diagram of the hollow fiber membrane system.
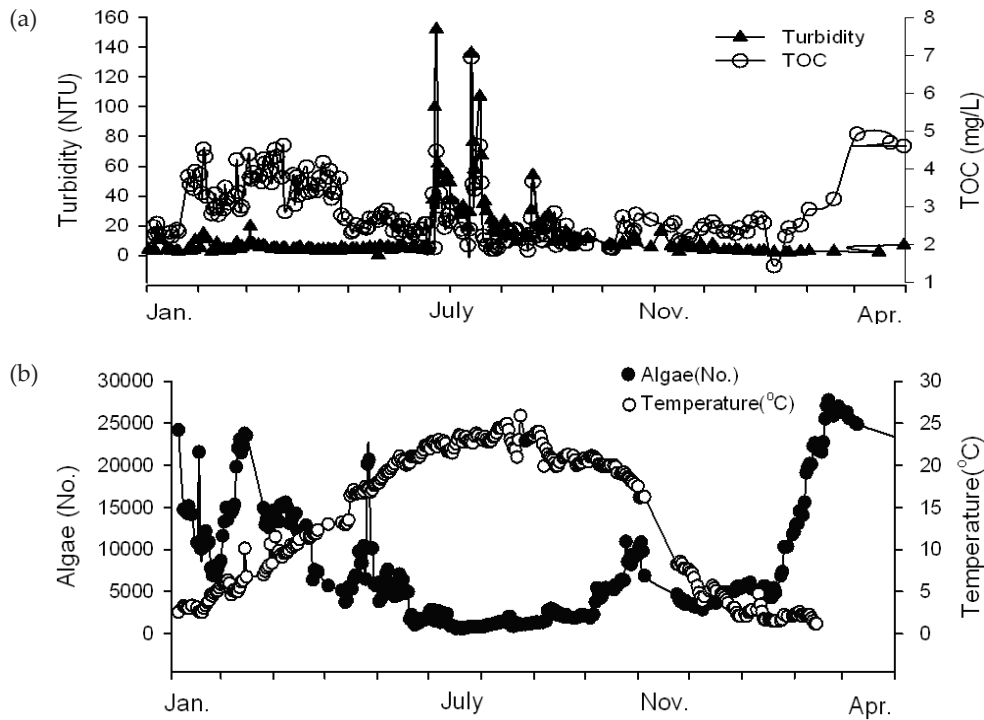
Fig. 3. Seasonal variations in the raw water quality: (a) Turbidity and TOC (b) Algae number and temperature.

Table 3
Characteristics of raw water quality in this study

Items	Average	Std. Dev.	Min.	Max.
Turbidity, NTU	13.28	20.07	150.00	2.02
Temperature, °C	14.00	8.12	1.16	25.89
TOC, mg/L	2.87	0.79	6.94	1.43
Algae no., cell/mL	7,404	6,921	306	27,750

slope of the linear region in a plot of AP vs. time, which corresponds to the cake filtration or the manipulation of Eq. (5). The fouling rate ranged from n.d. (not detected) to 14.16 m^{-2}. Fig. 4 shows the changes in the fouling rate in the pressurized MF system. The extent of fouling significantly depended on the raw water quality. The fouling rate remained high (between April and May) because of the increased concentration of organics and the algae number. It rapidly increased to a level about the middle of July because of high turbidity. From October, the fouling rate continuously increased because of the increased concentration of organics, the algae number, and the decreased water temperature. Accordingly, the fouling rate was found to be sensitive to the seasonal variation in raw water quality. Therefore, it can be concluded that the fouling rate properly reflects the seasonal differences in the raw water quality.
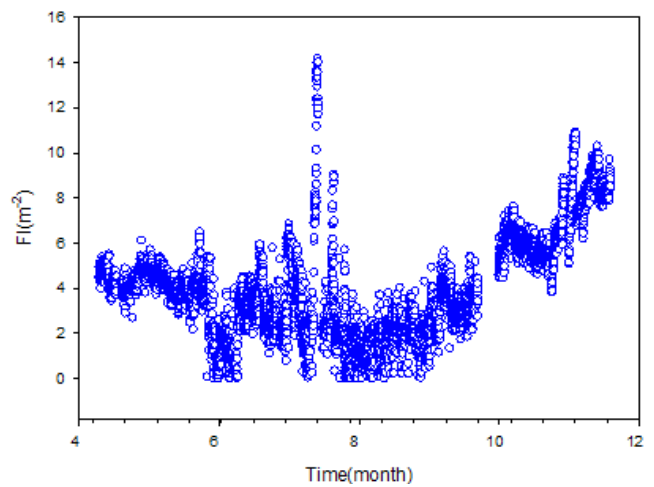
Fig. 4. Changes in the fouling rate in the pressurized MF system.

4.3. Prediction of membrane performance using the ANN model

STATISTICA, statistics program automatically determines the optimum network structure so it would become the minimum value of R^2. The structure of the ANN that was used in this study to predict the fouling rate with five input and six hidden nodes is shown in Fig. 5a, and the structure of the other ANN that was used in this study to predict the permeability with five input and seven hidden nodes is shown in Fig. 5b.

4.4. Fitting of ANN to the fouling rate and permeability dataset

Figs. 6 and 7 show the observed and predicted values for the fouling rate and permeability in the pilot-scale membrane system, respectively. Figs. 5a and 6a, in particular, show a comparison of the observed and predicted values according to the operating time. Figs. 5b and 6b, on the other hand, show a comparison of the fouling rate and permeability in the experiment with the simulated data. The predicted values from the model match the experiment values very well.

The performances of the ANN model were evaluated using the root mean squared error (RMSE) and the correlation coefficient (R^2). The results of the RMSE and R^2 statistical criteria for the evaluation of the ANN model are presented in Table 4.

The ANN models showed high strength and a linear-relationship direction between the predicted data and the
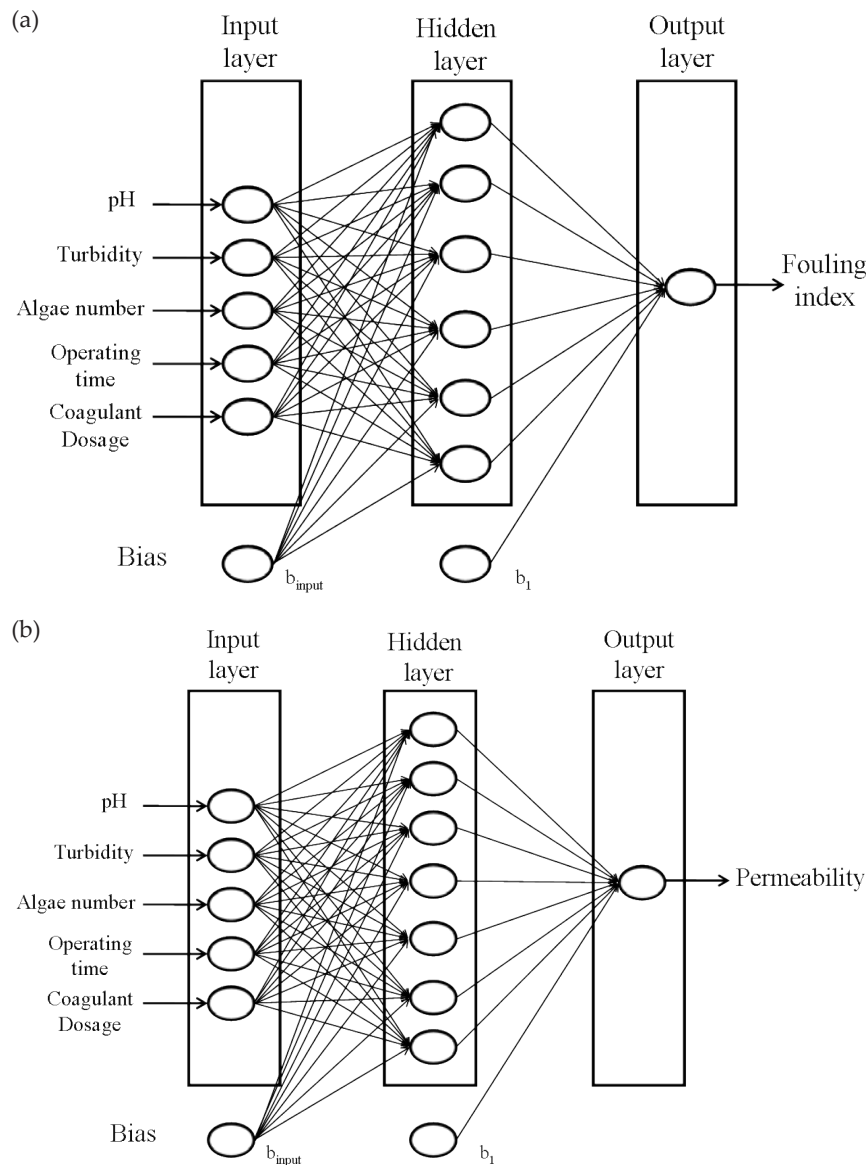
Fig. 5. Architecture of the neural networks for predicting the fouling rate and permeability: (a) Five input neurons, six hidden layers, and one output neuron; (b) Five input neurons, seven hidden layers, and one output neuron.
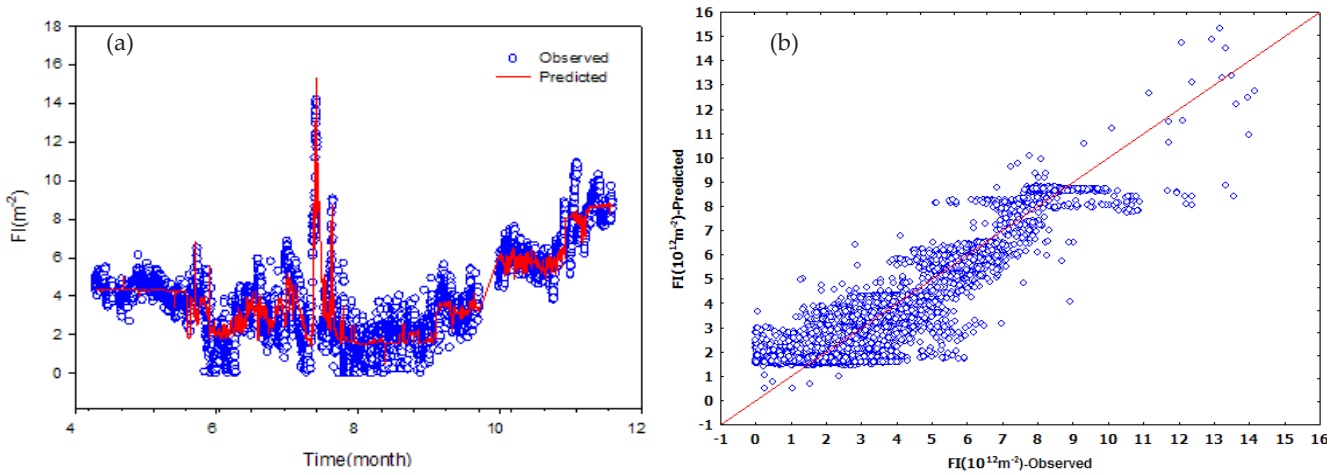
Fig. 6. Comparison of the ANN model fit with the experiment data on the fouling rate. The correlation of the experiment observations with the neural-network predictions is shown in (a) panel (b) shows the comparison of the observation data with the neural-network predictions according to the operating time
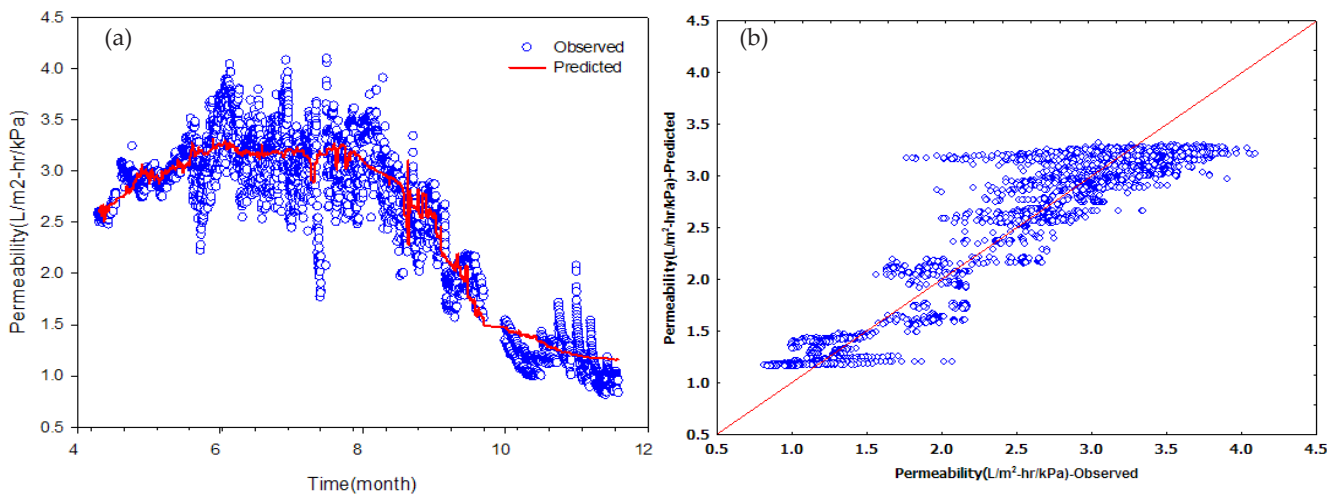
Fig. 7. Comparison of the ANN model fit with the experiment data on permeability. The correlation of the experiment observations with the neural-network predictions is shown in (a) panel (b) shows the comparison of the observation data with the neural-network predictions according to the operating time.

Table 4
Statistical criteria for the evaluation of the ANN model

Item	Partition	R^2	RMSE
Fouling rate	Train	0.91	0.886
	Test	0.92	0.867
Permeability	Train	0.93	0.253
	Test	0.94	0.239

observed data. This suggests that the ANN model has potential for use in the prediction of membrane fouling in pilot-scale systems.

Fig. 8 shows the RMSE and the number of iterations. A sharp drop in the RMSE in the first a few iterations (fast training) is shown. The training cycles stopped after 85 and 65 iterations, with an RMSE value of 0.01 respectively.

5. Conclusions

The seasonal differences in the raw-water quality significantly affected membrane fouling in Korea. The fouling rate based on the cake filtration model is effective for quantitatively estimating the fouling degree of a pressurized MF system in constant flux. The prediction of the fouling rate using the artificial neural network model is effective for the prediction of plant operation
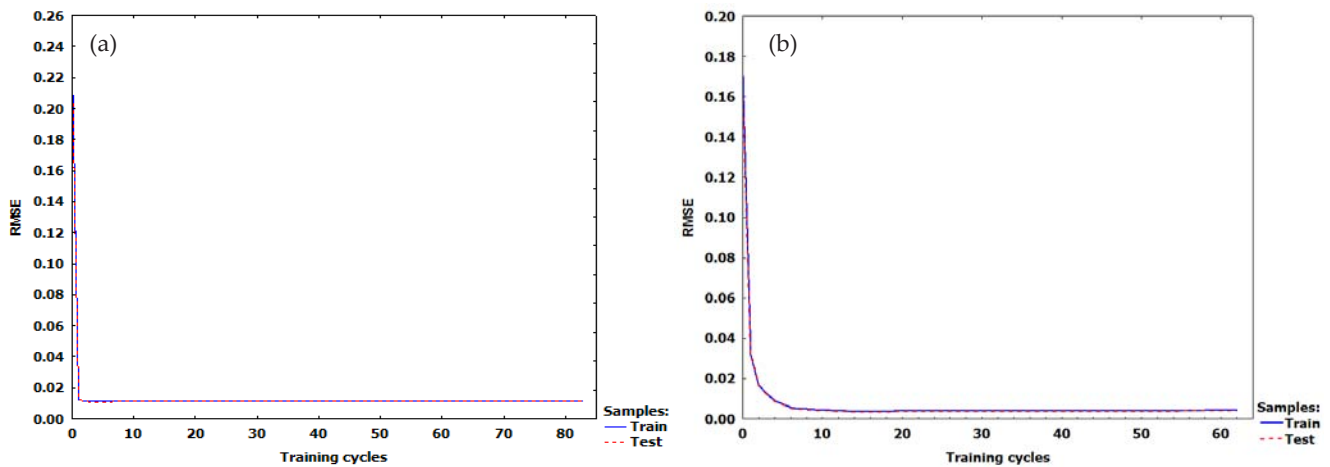
Fig. 8. RMSE as a function of the number of iterations (a) Fouling rate; (b) Permeability.

data, which have a sharp contrast in raw water quality by season. It is expected that the optimum operation conditions can be reduced by regulating the coagulant injection quantity and the backwash cycle and intensity, among others, based on the real time data of raw water quality, through the prediction of the fouling rate using the artificial neural network model.

Symbols

A	—	Membrane area
C_0	—	Concentration of pollutants
$I = \alpha C_0$	—	Fouling index
J	—	Permeate flux
ΔP	—	Transmembrane pressure
R_c	—	Cake resistance
R_m	—	Membrane resistance
t	—	Operating time
V	—	Filtration volume
α	—	Specific cake resistance
μ	—	Viscosity

References

[1] L.J. Zeman and A.L. Zydney, Microfiltration and Ultrafiltration, Marcel Dekker, New York, 1993.

[2] J.N. Mhurchuú and G. Foley, Dead-end filtration of yeast suspensions: Correlating specific resistance and flux data using artificial neural networks, J. Membr. Sci., 281 (2006) 325–333.

[3] K.J. Hwang and Y.J. Wu, Flux enhancement and cake formation in air-sparged cross-flow microfiltration, Chem. Eng. J., 139 (2008) 296–303.

[4] G.R. Shetty and S. Chellam, Predicting membrane fouling during municipal drinking water nanofiltration using artificial neural networks, J. Membr. Sci., 217 (2003) 69–86.

[5] G.B. Sahoo and C. Ray, Predicting flux decline in crossflow membranes using artificial neural networks and genetic algorithms, J. Membr. Sci., 283 (2006) 147–157.

[6] M. Cheryan, Ultrafiltration and Microfiltration Handbook, Technomic, Lancaster, Pa., 1998.

[7] F.E. Siobhan, Development of the MFI-UF in constant-flux filtration, Desalination, 161 (2004) 103–113.

[8] K.L. Fox, R.R. Henning and J.H. Reed, A neural-network approach towards intrusion detection, Proc. 13th National Computer Security Conference, 1990.

[9] D. Hammerstrom, Neural networks at work, IEEE Spectrum, 1993, pp. 26–53.